THE JOURNAL OF BIOLOGICAL CHEMISTRY VOL. 285, NO. 51, pp. 39994–40003, December 17, 2010

Mitotic Inhibition of GRASP65 Organelle Tethering Involves Polo-like Kinase 1 (PLK1) Phosphorylation Proximate to an Internal PDZ Ligand*

Received for publication, September 28, 2010 Published, JBC Papers in Press, October 11, 2010, DOI 10.1074/jbc.M110.189449

Debrup Sengupta and Adam D. Linstedt[1]

From the Department of Biological Sciences, Carnegie Mellon University, Pittsburgh, Pennsylvania 15213

GRASP65 links cis-Golgi cisternae via a homotypic, N-terminal PDZ interaction, and its mitotic phosphorylation disrupts this activity. Neither the identity of the PDZ ligand involved in the GRASP65 self-interaction nor the mechanism by which phosphorylation inhibits its interaction is known. Phospho-mimetic mutation of known cyclin-dependent kinase 1/cyclin B sites, all of which are in the C-terminal "regulatory domain" of the molecule, failed to block organelle tethering. However, we identified a site phosphorylated by Polo-like kinase 1 (PLK1) in the GRASP65 N-terminal domain for which mutation to aspartic acid blocked tethering and alanine substitution prevented mitotic Golgi unlinking. Further, using interaction assays, we discovered an internal PDZ ligand adjacent to the PLK phosphorylation site that was required for tethering. These results reveal the mechanism of phosphoinhibition as direct inhibition by PLK1 of the PDZ ligand underlying the GRASP65 self-interaction.

The Golgi apparatus, which exists as a single copy organelle in higher eukaryotes, fragments in a stepwise fashion into vesicles and vesicle clusters that are partitioned into daughter cells during mitosis (1–6). The organelle is present during interphase as interconnected ministacks forming a ribbon-like membrane network. In late G_2 phase of the cell cycle, the ribbon becomes unlinked resulting in multiple ministacks clustered around the microtubule organizing center (6–9). From prophase to metaphase the unlinked ministacks vesiculate, and the vesicles largely disperse with some vesicles aggregating to form vesicle clusters (10, 11). Interestingly, in addition to being a consequence of mitotic regulation, Golgi fragmentation also appears to play a causal role. Failure of Golgi unlinking in G_2 phase delays mitotic entry possibly serving as a checkpoint (5, 6, 12).

Aspects of the mechanism underlying Golgi unlinking are beginning to emerge in part due to a better understanding of Golgi ribbon formation (8, 9, 13). Ribbon formation requires GRASP65 and GRASP55, which are localized to cis and medial Golgi cisternae, respectively (8, 9). GRASP65 is associated with the membrane via both binding to GM130 and insertion of its myristoylated N terminus (8, 14). GRASP55 binds golgin-45 and other proteins on the Golgi and is myristoylated and palmitoylated (15, 16). Each GRASP self-associates, and this underlies homotypic tethering of adjacent ministacks (8, 9, 17–19). Oligomer formation depends on the conserved tandem PDZ-like domains at the N terminus referred to as the GRASP domain, and point mutations in the predicted binding groove of the first PDZ domain of GRASP65, PDZ1, block tethering activity and Golgi ribbon formation (17, 19). Experiments suggest that GRASP65 is oriented on the membrane in such a way that it favors self-interaction in *trans* (20), but the identity of the PDZ ligand is unknown.

Cyclin-dependent kinase 1/cyclin B (CDK1),[2] a MEK/ERK cascade, and Polo-like kinase 1 (PLK1), contribute to mitotic Golgi breakdown, and each phosphorylates one or both GRASP proteins (4, 6, 12, 21–23). ERK directly phosphorylates GRASP55, and inhibition of its upstream activator MEK1 blocks both GRASP55 phosphorylation and G_2 phase Golgi unlinking (6, 9, 21). Further, mutation of ERK phosphorylation sites in GRASP55 to mimic the phosphorylated state blocks GRASP55 activity in both Golgi ribbon formation and self-association (9). Thus, GRASP55 phosphorylation drives Golgi unlinking by blocking *trans* complexes involved in membrane tethering. This model also applies to GRASP65, which is directly phosphorylated at multiple sites by CDK1, ERK, and PLK1, and phosphorylation blocks its homo-oligomerization *in vitro* (24–29). However, the direct involvement of these kinases and their phosphorylation sites has not been established. The known sites are outside the GRASP domain in a long nonconserved segment referred to as the serine-proline-rich regulatory domain (17, 21, 24, 27). It is unclear how phosphorylation of the C-terminal domain regulates tethering activity of the N-terminal self-interacting domain.

In considering GRASP65 phosphorylation by multiple kinases we were intrigued that the PLK family of kinases initially binds substrate and becomes activated through their Polo box domains. The Polo box domain binds to a phosphoserine/threonine motif that includes proline, S(pS/pT)P, and then the kinase can phosphorylate distant sites (30–32). Because CDK1 and ERK phosphorylate serine or threonine residues adjacent to proline it could be that GRASP phosphorylation by these kinases creates a binding site in the C-terminal domain for PLK1. Indeed, PLK1 binds the GRASP65 C-terminal domain under mitotic conditions (29). Thus, recruitment of PLK1 to the GRASP C-terminal domain could activate

* This work was supported, in whole or in part, by National Institutes of Health Grant GM-56779 (to A. D. L.).

[1] To whom correspondence should be addressed: 4400 5th Ave., Pittsburgh, PA 15213. E-mail: linstedt@cmu.edu.

[2] The abbreviations used are: CDK1, cyclin-dependent kinase 1/cyclin B; PLK1, Polo-like kinase 1.

PLK1 for phosphorylation of additional sites, perhaps including the GRASP domain to block tethering directly.

To test whether either CDK1 or PLK1 directly inhibits GRASP65-mediated organelle tethering, we mutated the known CDK1/ERK sites and mapped and mutated a novel PLK1 site and assayed the tethering activity of GRASP65 using a recently described assay on the outer membrane of mitochondria (19). Only a phospho-mimic mutation of the PLK1 site blocked tethering, and the same mutation blocked Golgi ribbon formation in a gene replacement assay. We also mapped the PDZ ligand underlying GRASP65 self-interaction and found that it was next to the PLK1 site. Altogether, the results support a model in which phosphorylation by PLK1 alters the activity of an adjacent internal PDZ ligand so that it can no longer bind the PDZ1 groove of a GRASP65 molecule on an apposing membrane.

MATERIALS AND METHODS

Reagents—Primary antibodies were as follows: anti-myc 9e10 (21), anti-phosphoserine (Zymed Laboratories), anti-His tag (Bethyl Laboratories), anti-phosphohistone-H3 (Upstate Cell signaling solutions), and anti-GM130 (8). MitoTracker (Invitrogen) was used to stain mitochondria as described (19). Olomoucine II and thymidine were from Sigma.

Constructs—G65^{7XD}-GFP-ActA was generated by sequential introduction of aspartic acid codons corresponding to residues Thr^{216}, Thr^{237}, Ser^{241}, Ser^{274}, Ser^{291}, Ser^{373}, and Ser^{397} into the human G65-myc construct (19) following the QuikChange protocol (Stratagene) and then by cloning the resulting GRASP65 sequence in frame into the NheI site of GFP-ActA (19). G65^{S189A}-GFP-ActA, G65^{S189D}-GFP-ActA, G65^{Y196A}-GFP-ActA, G65^{S189A}-myc, G65^{S189D}-myc, G65^{Y196A}-myc, and G65^{LK55,56NI}-His were generated using QuikChange to change the indicated codons in the parent vectors. GST-G65$^{173–212}$ was generated from GST-G65 (19) by deleting codons for residues 7–172 and adding a stop codon at residue 213. GST-G65$^{192–212}$, GST-G65$^{200–212}$, and GST-G65$^{205–212}$ were made from GST-G65$^{173–212}$ using a loop out protocol. GST-G65$^{173–191}$ and GST-G65$^{192–204}$ were made by adding stop codons at the indicated positions of GST-G65$^{173–212}$ and GST-G65$^{192–212}$, respectively. Alanine scan mutations of GST-G65$^{192–212}$ were made by using QuikChange to substitute alanine codons at the indicated positions. For His-PDZ1 (residues 7–108) and His-PDZ2 (residues 106–197) the indicated GRASP65 sequence was cloned between BamHI and EcoRI sites of pRSET-B.

Cell Culture and Transfection—HeLa cells were grown in minimal essential medium (Sigma) containing 10% fetal bovine serum (Atlanta Biological) and 100 units/ml penicillin and streptomycin (Sigma) and maintained at 37 °C in a 5% CO_2 incubator. Transient transfection was carried out with jetPEI^{TM} (Polyplus) according to the manufacturer's specifications. After 24 h, the cells were labeled with 15 nM MitoTracker for 30 min and fixed. Knockdown of GRASP65 by RNA interference and gene replacement was performed as described (19). To score G_2 and M-phase Golgi morphology, cells expressing GFP-GalNAc-T2 were plated at 50% confluence and subjected to double thymidine arrest as described (6). At 5 h after release from the second thymidine block, the medium was adjusted to 10 μM olomoucine II for another 6 h to arrest cells in late G_2. For M phase, the olomoucine II was washed out, and the cells were recultured for another 45 min.

Image Capture and Analysis—Imaging was performed using a spinning disk confocal scan head equipped with three-line laser and independent excitation and emission filter wheels (PerkinElmer Life Sciences) and a 12-bit Orca ER digital camera (Hamamatsu) mounted on an Axiovert 200 microscope with a 100×, 1.4 NA oil-immersion objective (Carl Zeiss MicroImaging). Sections at 0.3-μm spacing were acquired using Imaging Suite software (PerkinElmer Life Sciences). Radial profile analysis was as previously described (19). Mitotic cluster volume was determined using the "Voxel Counter" plug-in of ImageJ (National Institutes of Health) after background subtraction to remove vesicular haze. Total volume was divided by the number of clusters from the "Particle Count" function of ImageJ to yield volume per cluster.

Protein Purification and Binding Assays—Full-length GRASP65 proteins (G65-His, G65^{LK55,56NI}-His, and G65^{S189A}-His) were purified after expression in BL21(DE3)-pLysS cells cotransformed with pBB131 encoding *N*-myristoyltransferase (33). Expression was induced by 1 mM isopropyl β-D-thiogalactopyranoside at 30°C for 4 h in the presence of 200 μM myristic acid. Purification on nickel-nitrilotriacetic acid beads (Invitrogen) was according to manufacturer's protocol. The preparations were then dialyzed against HK buffer (10 mM HEPES, 100 mM KCl, 1.4 mM β-mercaptoethanol) and further purified on a Superdex-200 gel filtration column attached to an FPLC (GE Healthcare). Fractions corresponding to a well formed peak eluting at 11 ml were collected and dialyzed against HKT binding buffer (HK adjusted to 0.5% Triton X-100 and 5% glycerol). GST-tagged GRASP65 peptides were purified as described previously (34) after expression in DH5α and induction using 1 mM isopropyl β-D-thiogalactopyranoside for 3–5 h at 30 °C. Binding was carried out in 100 μl of HKT binding buffer containing 5 μg of each purified protein, unless indicated otherwise. After 3 h at 4 °C, glutathione-agarose beads (5 μl), which had been blocked with 10 μg of BSA, were added to the reaction for 1 h. Proteins recovered on the beads after three washes with HKT were analyzed by immunoblotting using the anti-His antibody.

PLK1 Phosphorylation Assay—Purified G65-His and G65^{S189A}-His were incubated with 200 ng of active PLK1 (Cell Signaling Technology) and 50 μM ATP in kinase buffer (5 mM MOPS, pH 7.2, 2.5 mM β-glycerophosphate, 1 mM EGTA, 4 mM $MgCl_2$, 0.05 mM DTT) at room temperature for 25 min. The samples were immunoblotted using the anti-phosphoserine antibody.

RESULTS

Phospho-mimic Mutations of GRASP65 CDK1/ERK Sites Do Not Block Tethering—To test whether CDK1 or ERK-mediated phosphorylation directly blocks tethering by GRASP65, we converted all potential CDK1 and ERK sites in the C-ter-

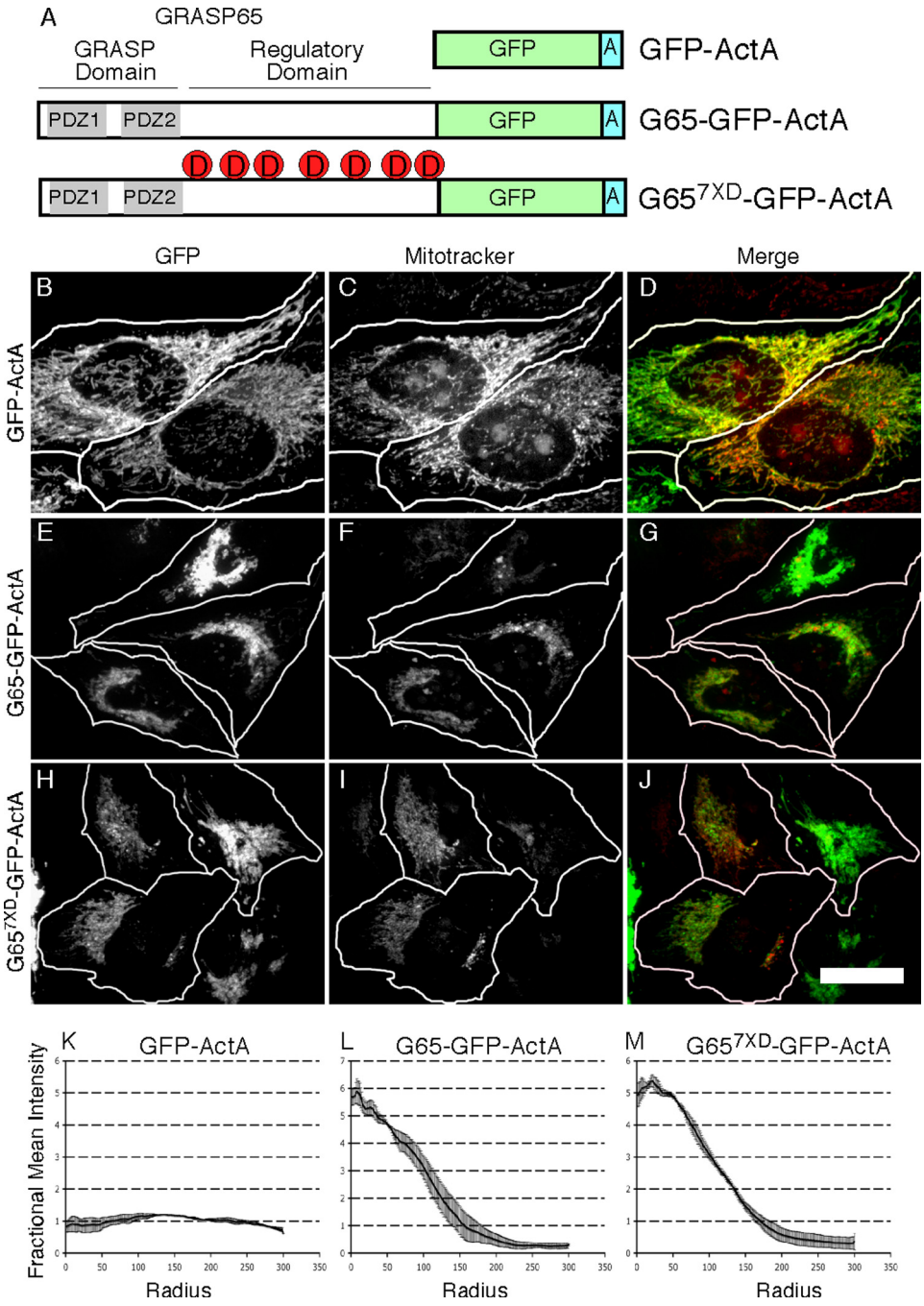

FIGURE 1. **Phospho-mimic mutations of mapped CDK1 sites of GRASP65 fail to block tethering.** *A*, schematic diagram of the constructs used is shown. *B–J*, HeLa cells expressing GFP-ActA (*B–D*), G65-GFP-ActA (*E–G*), and G65^{7XD}-GFP-ActA (*H–J*) were analyzed 24 h after transfection using MitoTracker to stain mitochondria (*C*, *F*, and *I*) and GFP to localize the transfected proteins (*B*, *E*, and *H*). A false-colored, merged image is also shown (MitoTracker and GFP are *red* and *green*, respectively). *Scale bar*, 10 μm. *K–M*, analysis was also carried out after a 30-min brefeldin A treatment. Radial profile plots show the spread of mitochondrial fluorescence starting from the centroid and extending to the cell periphery for cells expressing GFP-ActA (*K*), G65-GFP-ActA (*L*), or G65^{7XD}-GFP-ActA (*M*). Values are averages corresponding to the fraction of total fluorescence present in each concentric circle drawn from the centroid ($n = 3$, S.E., >15 cells/experiment).

minal domain to aspartic acid to mimic the phosphorylated state. The resulting construct, G65^{7XD}-GFP-ActA, also contained GFP and the mitochondrial targeting sequence ActA appended to its C terminus (Fig. 1*A*). As described previously (19), a control GFP-ActA sequence localized to the mitochondrial outer membrane yielding a "hyphal" pattern colocalized with mitochondrial markers such as MitoTracker (Fig. 1, *B–D*). In contrast, G65-GFP-ActA induced mitochondrial clustering (Fig. 1*E*-G), which was previously shown to involve its self-interaction in *trans* (19). Mitochondrial clustering was also evident for G65^{7XD}-GFP-ActA (Fig. 1, *H–J*). These results were quantified for multiple cells by determining the fluorescence distribution in concentric circles emanating from the centroid of mitochondrial fluorescence. Whereas the radial profile of fluorescence in control cells was uniform, there was strong clustering of the fluorescence in cells expressing G65-

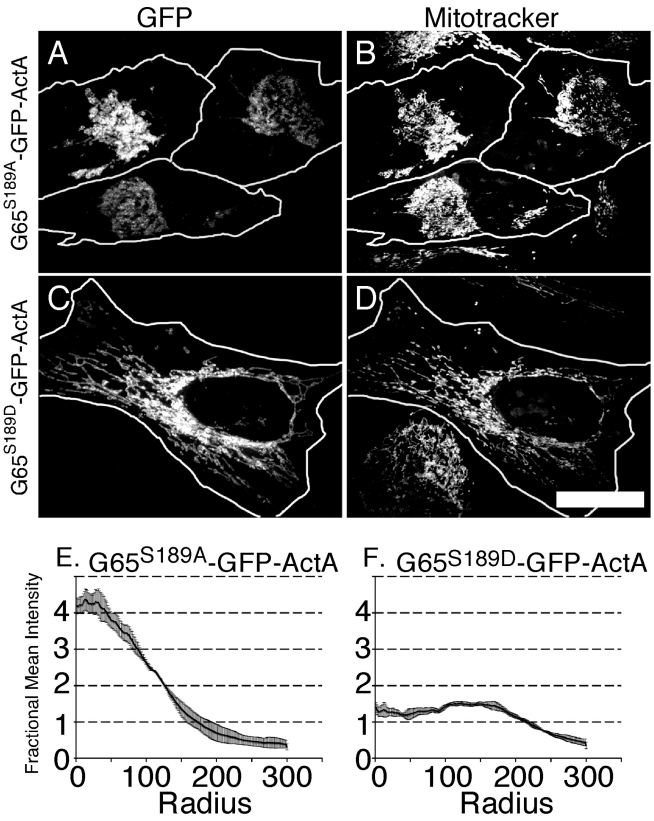

G

	S189
Human	^{180}PNAAWGGEG**S**LGCGIGYGYLHRIPTQPPS
Rat	^{179}PNAAWGGEG**S**LGCGIGYGYLHRIPTQPSS
Mouse	^{179}PNAAWGGEG**S**LGCGIGYGYLHRIPTQPSS
Dros.	^{180}PNTAWGGEGALGCGIGFGYLHRIPVQAEP

FIGURE 2. **Phospho-mimic mutation S189 inhibits GRASP65 tethering activity.** Cells expressing G65^{S189A}-GFP-ActA (*A*, *B*) and G65^{S189D}-GFP-ActA (*C*, *D*) were BFA-treated and analyzed using Mitotracker to stain mitochondria (*B*, *D*) and GFP fluorescence (*A*, *C*) to localize the transfected proteins. *Bar* = 10 μm. Radial profile plots show the spread of mitochondrial fluorescence for cells expressing G65^{S189A}-GFP-ActA (*E*) or G65^{S189D}-GFP-ActA (*F*). Also shown is a sequence alignment indicating conservation of S189 in higher eukaryotes (*G*).

GFP-ActA and G65^{7XD}-GFP-ActA (Fig. 1, *K*–*M*). Thus, phospho-mimic mutations of the GRASP65 CDK1 sites did not block tethering, prompting us to search for sites elsewhere in the molecule that directly inhibit its organelle tethering activity.

PLK1 Phosphorylation of GRASP65 Ser^{189} Blocks Tethering and Golgi Ribbon Formation—To test whether PLK1 might inhibit GRASP65 tethering directly we identified and mutated three phosphorylation sites matching the PLK1 substrate consensus sequence E*X*S/TΦ, where *X* is any residue and Φ is hydrophobic (35). One of these, Ser^{189}, yielded no effect when mutated to alanine to prevent phosphorylation (Fig. 2, *A* and *B*) but potently blocked clustering when mutated to aspartic acid to mimic phosphorylation (Fig. 2, *C* and *D*). The result was confirmed for cell populations using the radial profile algorithm (Fig. 2, *E* and *F*). The fact that alanine substitution at the same position did not interfere argues that loss of tethering for S189D was due to mimicking the phosphorylated state rather than perturbed protein folding. Interestingly,

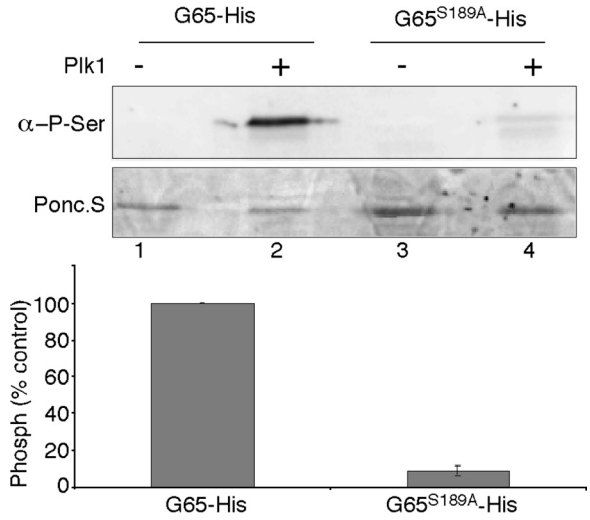

FIGURE 3. **PLK1 phosphorylates GRASP65 Ser^{189}.** *Upper*, the reactivity to phosphoserine-specific antibody was determined for equivalent amounts (1 μg) of purified G65-His and G65^{S189A}-His after incubation in the presence or absence of active PLK1 kinase. Ponceau S staining shows amount of protein present. *Lower*, phosphorylation was quantified by determining the signal intensity normalized to G65-His ($n = 3$, ± S.D., $p < 0.01$).

multiple sequence alignment indicates that Ser^{189} is conserved in organisms with mitotically disassembled Golgi ribbons but not others (Fig. 2*G*).

Because phosphorylation of Ser^{189} had not been described previously, we tested for phosphorylation of this site by PLK1. Purified proteins were used rather than a cell-based assay so that we could test for direct phosphorylation. Further, in cells, GRASP65 is phosphorylated on many sites by multiple kinases, making it difficult to test a single site. GRASP65 was His-tagged at its C terminus and purified out of bacteria using nickel-agarose beads. The purified preparation was incubated with ATP in the presence and absence of purified PLK1. Phosphorylation was detected when PLK1 was present using an anti-phosphoserine antibody, and this was inhibited by the S189A mutation (Fig. 3). Thus, Ser^{189} of GRASP65 is phosphorylated directly by PLK1.

Having mapped a PLK1 phosphorylation site on GRASP65 that inhibits its tethering activity, we sought to test its role in Golgi ribbon formation using gene replacement after siRNA-mediated knockdown of GRASP65. GRASP65 knockdown and rescue were carried out as described previously (19). Cells depleted of GRASP65 exhibited fragmented Golgi ribbons, and this phenotype was rescued by expressing a siRNA-resistant version of GRASP65 tagged at its C terminus with the myc epitope (Fig. 4, *A* and *B*). In contrast, a rescue construct containing the S189D substitution, G65^{S189D}-myc, failed to rescue (Fig. 4, *C* and *D*). This construct appeared stably targeted to the fragmented Golgi membranes, suggesting proper folding. Further, alanine substitution at the same site yielded a construct, G65^{S189A}-myc, which promoted rescue to the same extent as wild type (Fig. 4, *E*–*G*). Thus, GRASP65 tethering activity is dependent on the phosphorylation state of Ser^{189}.

Phosphorylation of GRASP65 Ser^{189} Is Required for Cell Cycle-dependent Golgi Unlinking and Fragmentation—PLK1 is activated late in the G_2 phase of the cell cycle (36, 37), the

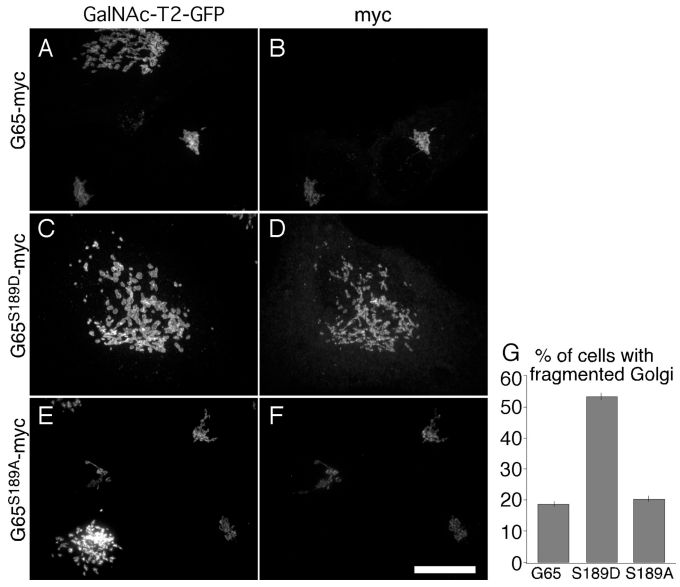

FIGURE 4. **Phospho-mimic GRASP65^{S189D} fails to rescue Golgi ribbon formation.** HeLa cells expressing GalNAcT2-GFP and transfected with GRASP65 siRNA and siRNA-resistant forms of G65-myc (*A*, *B*), G65^{S189D}-myc (*C*, *D*), or G65^{S189A}-myc (*E*, *F*) were analyzed to assess Golgi morphology (*GalNAcT2-GFP*) and replacement construct expression (*myc*). *Bar* = 10 μm. Percentage of cells (*G*) expressing G65-myc, G65^{S189D}-myc or G65^{S189A}-myc exhibiting a fragmented Golgi after knockdown with GRASP65 siRNAs (±SEM, $n = 4$, >100 cells in each, $p < 0.01$).

time of Golgi unlinking (5, 6). To test whether GRASP65 phosphoinhibition at Ser^{189} is required for Golgi unlinking we assayed Golgi unlinking in cells expressing GRASP65-myc, G65^{S189A}-myc, and G65^{S189D}-myc. Synchronized cells were arrested in late G_2 using olomoucine II, which is an inhibitor of CDK1. Consistent with previous work (6), fragmented Golgi ribbons were observed in 60% of control cells and also cells expressing wild-type G65 (Fig. 5, *A*, *B*, and *G*). Cells expressing G65^{S189D}-myc also exhibited unlinked Golgi ribbons (Fig. 5, *C*, *D*, and *G*), as was expected given that this construct lacked tethering activity as shown above. In contrast, only 35% of cells expressing G65^{S189A}-myc had fragmented ribbons (Fig. 5, *E*–*G*). This finding implies that phosphorylation of the GRASP65 PLK1 site, Ser^{189}, is required for late G_2 unlinking of the Golgi ribbon.

Because CDK1-mediated phosphorylation of GRASP65 perturbs mitotic Golgi fragmentation, causing accumulation of larger mitotic Golgi clusters (24, 38), we tested whether mutation of the PLK1 site Ser^{189} might have a similar effect. Average cluster volume was determined in mitotic cells expressing G65-myc or G65^{S189A}-myc. Indeed, mitotic cells expressing G65^{S189A}-myc, identified using anti-myc and anti-phosphohistone H3 antibodies, had mitotic Golgi clusters that were 1.7-fold larger on average than those in the control cells (Fig. 6).

The S189D Phospho-mimic Mutation Does Not Affect GM130 Binding—GRASP65 is targeted to the Golgi by using its second PDZ-like domain (PDZ2) to bind the C-terminal PDZ ligand of GM130 (20, 39). Although Ser^{189} is near the GM130 binding site, G65^{S189D}-myc was Golgi-localized upon expression (Figs. 4, *C* and *D*, and 5, *C* and *D*), suggesting that the phosphorylation of Ser^{189} does not interfere with GM130

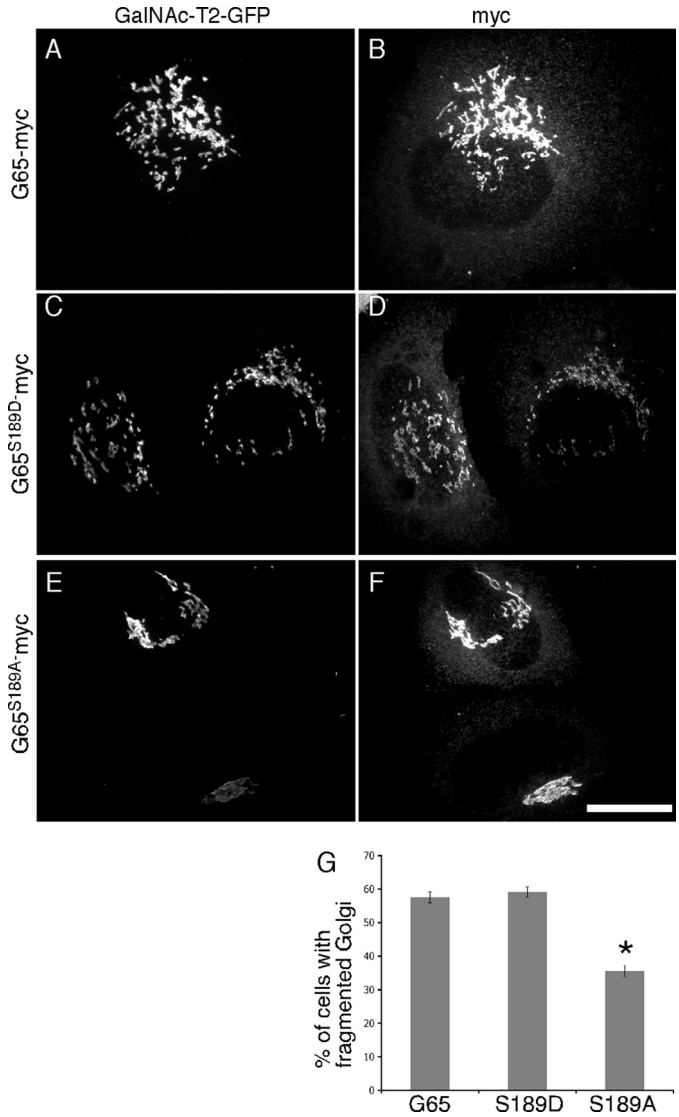

FIGURE 5. **Evidence that PLK1 phosphorylation of GRASP65 is required for late G_2 unlinking.** *A*–*F*, G65-myc (*A* and *B*), G65^{S189D}-myc (*C* and *D*), and G65^{S189A}-myc (*E* and *F*) were transiently transfected, and the cells were synchronized in late G_2 phase by a 5-h release from thymidine and then a 6-h treatment with olomoucine II. Expressing cells were identified by myc staining (*B*, *D*, and *F*) and the Golgi was analyzed based on GalNAc-T2-GFP (*A*, *C*, and *E*). *Scale bar*, 10 μm. *G*, the percentage of cells expressing G65-myc, G65^{S189D}-myc, and G65^{S189A}-myc and exhibiting an unlinked Golgi was quantified (±S.E., $n = 4$, >100 cells in each, $p < 0.01$).

binding. To confirm this finding, we used recruitment to mitochondria as an interaction test. As expected, the G65-GFP-ActA construct localized to mitochondria, induced mitochondrial clustering, and, because it binds GM130, recruited GM130 to the mitochondria (Fig. 7, *A*–*C*). Brefeldin A was used in these experiments to disassemble the Golgi complex. Although G65^{S189D}-GFP-ActA failed to induce clustering, GM130 recruitment was evident on the dispersed mitochondria (Fig. 7, *D*–*F*). Thus, the S189D phospho-mimic construct binds GM130, and its loss of tethering activity is not due to impaired interaction with GM130.

An Internal PDZ Ligand-binding GRASP65 PDZ1 Is Adjacent to Ser^{189}—GRASP65 self-association during tethering involves its first PDZ-like domain, PDZ1, binding to an

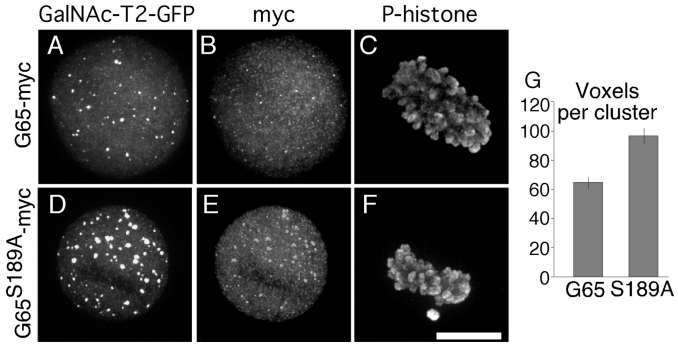

FIGURE 6. **Evidence that GRASP65 phosphorylation by PLK1 is required for mitotic Golgi disassembly.** Cells transiently transfected with G65-myc (*A–C*) or G65^{S189A}-myc (*D–F*) were synchronized in M-Phase by thymidine release into olomoucine II for 6 h followed by 45 min release from olomoucine II. Mitotic cells were identified by phospho-histone staining (*C*, *F*), expressing cells were identified by myc staining (*B*, *E*), and Golgi morphology was observed by GalNAc-T2 GFP florescence (*A*, *D*). *Bar* = 10 μm. Mitotic Golgi cluster size (*G*) was determined using the ImageJ "Voxel counter" plug-in based on GalNAcT2-GFP florescence (±SEM, $n = 3$, >15 cells in each, $p < 0.01$).

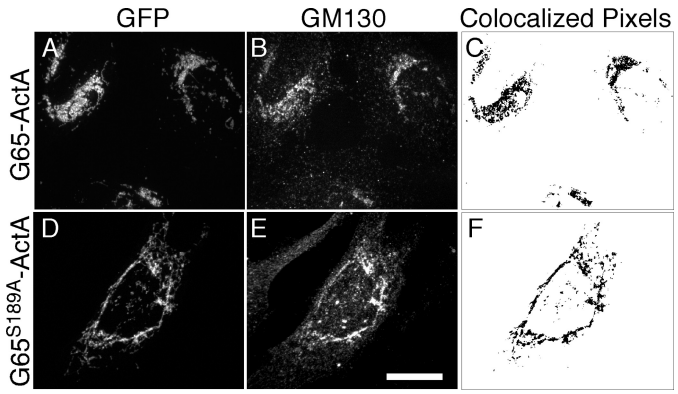

FIGURE 7. **Phospho-mimic GRASP65^{S189D} retains GM130 binding.** HeLa cells expressing G65-GFP-ActA (*A–C*) or G65^{S189D}-GFP-ActA (*D–F*) were BFA-treated for 30 min to disassemble the Golgi apparatus and processed to reveal GFP fluorescence (*A*, *D*) and GM130 staining (*B*, *E*). Maps of colocalized pixels indicating GM130 recruitment are also shown (*C*, *F*). *Bar* = 10 μm.

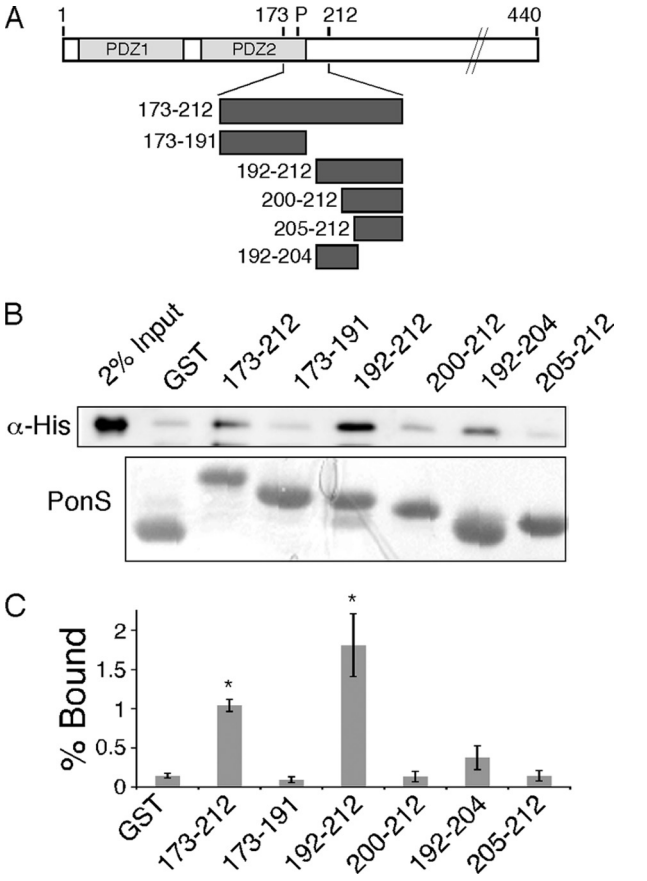

FIGURE 8. **Residues 192–212 bind full-length GRASP65.** *A*, schematic depicts GRASP65 GST fusion proteins tested for binding. Equivalent amounts (5 μg) of each fusion protein were incubated with 5 μg of purified G65-His for 3 h, and complexes were recovered on glutathione-agarose beads. G65-His binding was determined by immunoblotting with anti-His tag antibody (*B*) and quantified (*C*) relative to a 2% loading control ($n = 3$, ±S.E.; *, $p < 0.05$).

unidentified ligand located within GRASP65 but outside of residues 85–167 (19). Because S189D blocked tethering, we asked whether residues surrounding Ser^{189} contain the ligand that binds PDZ1. An *in vitro* binding assay was established in which purified His-tagged GRASP65, G65-His, was incubated with a series of purified, GST-tagged peptides from this region of GRASP65 (Fig. 8*A*). Significantly, the sequence stretch 173–212 bound GRASP65 at levels above background, and bisection of this stretch yielded strong binding by the C-terminal half, residues 192–212 (Fig. 8*B*). This was confirmed by quantification of multiple experiments (Fig. 8*C*). Further deletions reduced binding to near background levels, but the weak binding of 192–204 compared with the lack of binding for 200–212 suggested that the activity resides in residues 192–199. As a test, we performed alanine-scanning mutagenesis of the 192–212 construct. Significantly, alanine substitution at residues Ile^{194}, Tyr^{196}, Tyr^{198}, or Leu^{199} specifically reduced or abolished binding to GRASP65 (Fig. 9), indicating that this stretch was responsible for the interaction.

Consistent with our results, internal ligands typically have a length requirement of greater than 10 residues and, within this stretch, a central cluster of about five residues whose side chains are essential (40–42). To test whether the stretch we identified was binding the GRASP65 PDZ1 groove, we mutated the predicted groove to block binding. Purified G65-His, with or without a L55N,K56I substitution that blocks tethering,[3] was incubated with the purified GST fusion containing GRASP65 residues 192–212. Mutation of the predicted PDZ1 groove significantly reduced binding relative to wild type (Fig. 10, *A* and *B*). As a further test, we asked whether the ligand sequence would specifically bind an isolated version of PDZ1. Indeed, the purified GST-tagged residues 192–212 bound purified His-tagged PDZ1 but not PDZ2 (Fig. 10*C*). This interaction was specific because binding to PDZ1 was blocked by alanine substitution of either Tyr^{196} or Tyr^{198} in the ligand sequence (Fig. 10*D*). Altogether, these experiments indicate that the sequence stretch IGYGYL functions as an internal PDZ ligand binding to PDZ1.

Next, we sought to determine whether the mapped ligand is required for GRASP65 tethering and Golgi ribbon forma-

[3] D. Sengupta and A. D. Linstedt, unpublished observations.

tion. To test tethering, we expressed a mitochondrially targeted version of GRASP65 containing a single point mutation that blocked the *in vitro* interaction, Y196A. The resulting construct, G65^{Y196A}-GFP-ActA was targeted to mitochondria but failed to induce clustering (Fig. 11*A*). Inhibition by Y196A was confirmed using the radial profile analysis on a population of cells (Fig. 11*B*). To test Golgi ribbon formation, we expressed the same mutated form of GRASP65 in cells lacking endogenous GRASP65 due to knockdown. Significantly, GRASP65 knockdown caused Golgi unlinking, and this phenotype was rescued by G65-myc but not G65^{Y196A}-myc (Fig. 11, *C–H*). The lack of activity in Golgi ribbon formation for this point mutation in the internal ligand sequence was confirmed by quantification (Fig. 11*I*).

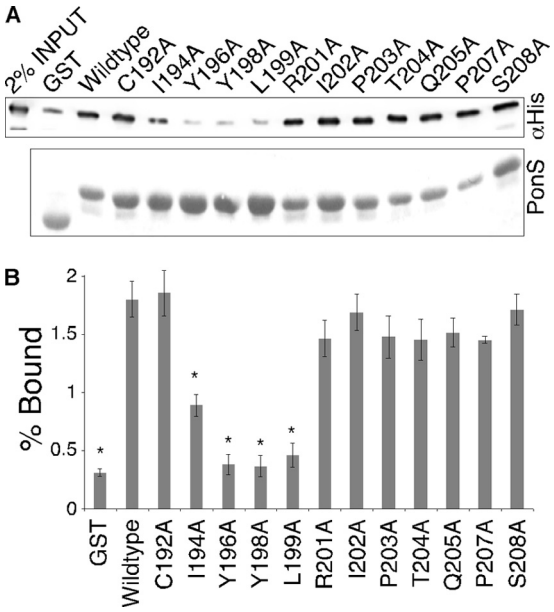

FIGURE 9. **Alanine scanning maps binding domain to residues 194–199.** GST alone or GST fused to GRASP65 residues 192–212 containing the indicated individual alanine substitutions was incubated with 5 μg of G65-His, and complexes were recovered on glutathione-agarose beads. G65-His binding was determined by immunoblotting with anti-His tag antibody (*A*) and quantified (*B*) relative to a 2% loading control ($n = 3$, $\pm$S.E.; *, $p < 0.01$).

DISCUSSION

The GRASP65 binding groove is known to be required for Golgi ribbon formation, but the corresponding ligand had not been identified (19). Similarly, PLK1 was shown to be important for mitotic Golgi disassembly and to bind and phosphorylate GRASP65, but the site of phosphorylation had not been mapped, and the significance of PLK1 phosphorylation of GRASP65 was not determined (24–26, 29). Our identification of the PDZ ligand mediating GRASP65 self-association and a nearby PLK1 site that functionally regulates the interaction significantly extends our understanding of Golgi ribbon formation and its unlinking at M phase. These findings support a model in which the binding groove of the first PDZ domain of GRASP65 on one membrane interacts with an internal ligand within the second PDZ domain of GRASP65 on an adjacent membrane to mediate organelle tethering; and, at the onset of mitosis, PLK1 blocks this interaction by phosphorylating a site next to the ligand (Fig. 12).

A 20-residue peptide at the end of the GRASP domain, Cys^{192}–Lys^{212}, bound the PDZ1 binding groove, and mutations within the stretch ^{194}IGYGYL^{199} blocked binding (Fig. 10), tethering (Fig. 11, *A* and *B*), and Golgi ribbon formation (Fig. 11, *C–I*). PDZ ligands are typically located at the C terminus and have been classified into several types defined largely by the four terminal residues of the protein. Although the GRASP65 ligand sequence most closely matches the type II PDZ ligand consensus sequence $\Phi X\Phi$, the GRASP65 sequence is internal. Internal ligands are less common, but sev-

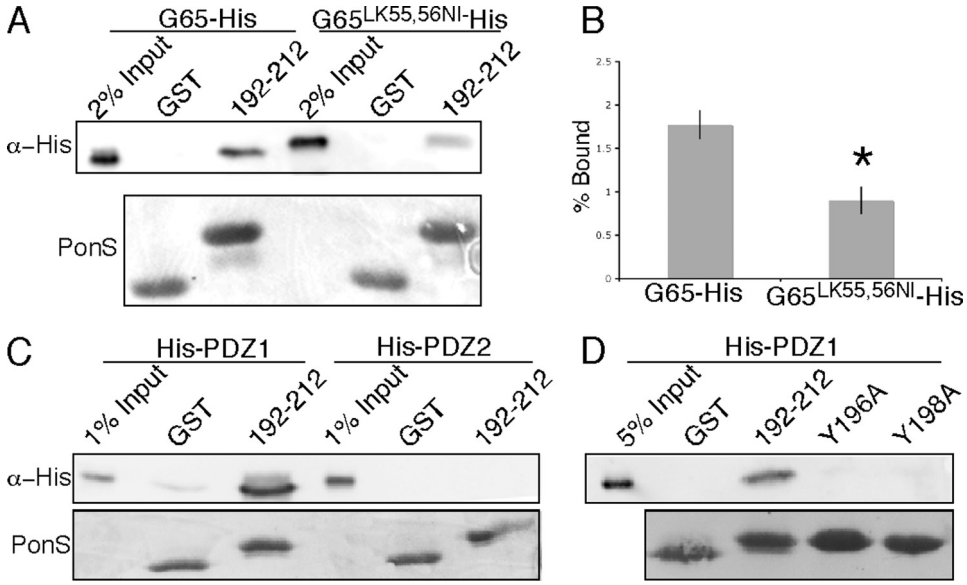

FIGURE 10. **Residues 192–212 bind the PDZ1 groove of GRASP65.** *A* and *B*, equivalent amounts (5 μg) of GST alone or GST fused to GRASP65 residues 192–212 were incubated with 2.5 μg of either G65-His or GRASP65^{LK55,56NI}-His, which had mutations in its predicted PDZ1 binding groove. Complexes were recovered on glutathione-agarose beads, and binding of the His-tagged GRASP65 proteins was determined by immunoblotting with anti-His tag antibody (*A*). The results were quantified (*B*) relative to a 2% loading control ($n = 4$, $\pm$S.E.; *, $p < 0.01$). *C*, GST alone or GST-192–212 (5 μg) was also incubated with 5 μg of the isolated GRASP PDZ domains, His-PDZ1 and His-PDZ2, and binding was compared with 1% loading controls. *D*, finally, GST alone or GST-192–212 (5 μg) with or without the indicated alanine substitutions was incubated with 5 μg of His-PDZ1 and compared with a 5% loading control.

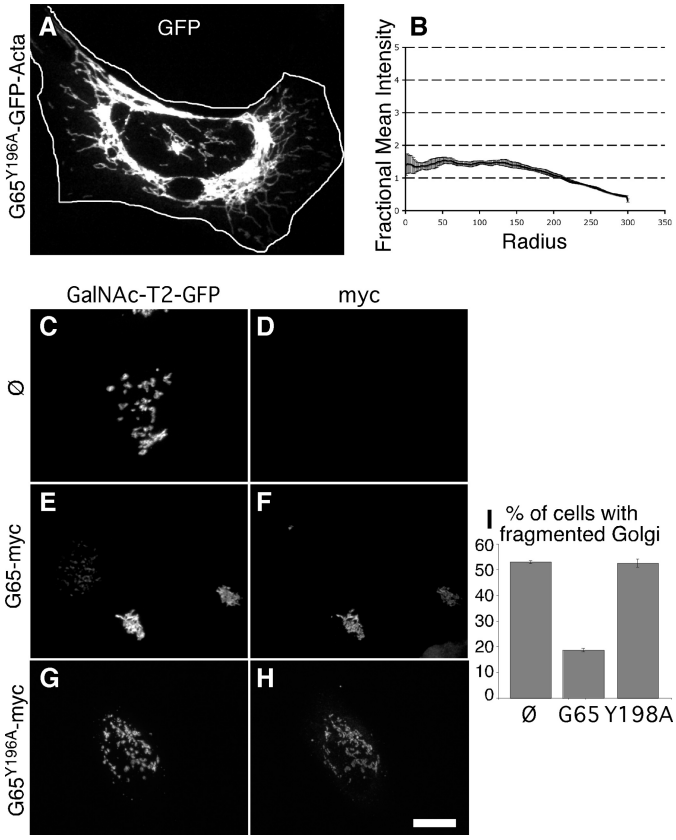

FIGURE 11. **Residue Y196 is required for GRASP65 tethering and Golgi ribbon formation.** Mitochondrial morphology was assessed in cells expressing G65^{Y196A}-GFP-ActA after a 30 min BFA treatment (*A*) and quantified using radial profile analysis (*B*). HeLa cells expressing GalNAcT2-GFP and transfected with GRASP65 siRNA only (*C*, *D*), or siRNA together with siRNA resistant forms of G65-myc (*E*, *F*), or G65^{Y196A}-myc (*G*, *H*) were analyzed to assess Golgi morphology (*C*, *E*, *G*) and replacement construct expression (*D*, *F*, *H*). *Bar* = 10 μm. Percentage of cells (*I*) expressing G65-myc or G65^{Y196A}-myc exhibiting a fragmented Golgi after knockdown with GRASP65 siRNAs (±SEM, $n = 4$, >100 cells in each, $p < 0.01$).

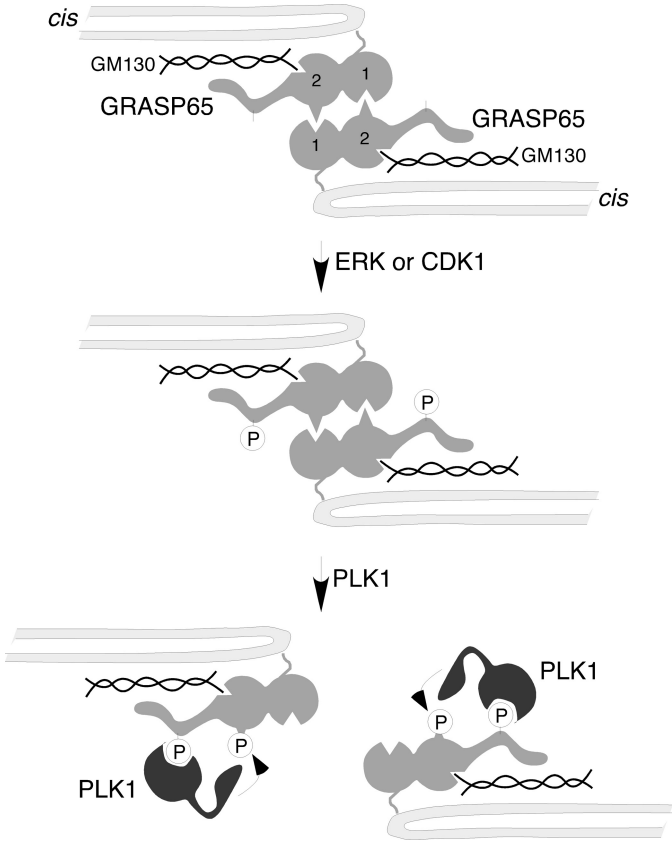

FIGURE 12. **Model depicts two-step phosphoinhibition.** GRASP65 is first shown tethering *cis* cisternae membranes. It is membrane-anchored by GM130 binding and myristic acid insertion and self-interacts via a reciprocal insertion of its ligand, present in PDZ2, into the groove of PDZ1. The unstructured C-terminal domain is then phosphorylated (presumably by ERK in late G_2 or CDK1 in M phase), creating a docking site for PLK1. Then the Polo box domain of PLK1 docks and the PLK1 catalytic domain phosphorylates Ser^{189} inactivating the PDZ ligand thereby inhibiting the tethering complex.

eral examples are well characterized, and different modes of interaction have been identified (42, 43). Some internal ligands contain an acidic residue that mimics the free C terminus of typical ligands, but these are not obligatory (40, 41, 43), and the GRASP65 ligand lacks this feature. Other internal ligands form a β-hairpin "finger-like" fold in which a β-strand mimics the canonical ligand interaction, and the sharp turn overcomes the steric constraints at the terminus of the ligand binding groove (42). This is also an unlikely mode of interaction for the GRASP65 internal ligand as secondary structure prediction suggests that it is unlikely to form a β-hairpin fold. A final mode of interaction involves conformational flexibility and seems most relevant. In this mode, glycines in internal ligands confer flexibility that neutralize the effect of steric barriers in the ligand binding groove (40, 41). The presence of two glycines in the GRASP65 internal ligand suggests that it uses a similar mechanism. The core and surrounding residues in the GRASP65 ligand sequence are conserved among GRASP proteins of higher eukaryotes, suggesting conservation of function. However, it is puzzling that GRASP55 has this sequence because it does not bind GRASP65. Determining the basis of specificity in GRASP homo-oligomer formation is an important future direction.

The presence of a PLK1 phosphorylation site, Ser^{189}, next to the PDZ ligand sequence suggests several possible inhibitory mechanisms. Binding of known internal ligands depends on both interactions within the ligand sequence as well as interactions involving adjoining residues (42). The latter increase the strength and specificity of binding and thus phosphorylation of adjoining residues could regulate binding. The C-terminal ligand in ErbB2 provides an example as its affinity for the Erbin PDZ domain is reduced by phosphorylation of a tyrosine residue outside the ligand sequence that, in its unphosphorylated state, contributes to binding (44). Alternatively, phosphorylation of Ser^{189} might alter presentation of the ligand on the surface of the molecule. In other words, adjoining residues including Ser^{189} may adopt a conformation in the folded PDZ2 domain that exposes the IGYGYL sequence, and phosphorylation of Ser^{189} may induce a conformational change in the ligand that blocks its access to the binding groove. This mode of regulation has been suggested for the NMDA receptor subunit NR2C, which is phosphorylated on a serine adjacent to its PDZ ligand sequence that binds PSD-95 (45). A final possibility is that Ser^{189} phosphorylation alters orientation of GRASP65 on the membrane. Dual anchoring of the GRASP domain to the membrane by myristic acid inser-

tion and GM130 binding facilitates *trans* pairing possibly by conferring a favorable orientation of the binding groove and/or ligand (20). As Ser^{189} is in the domain that binds GM130, its phosphorylation could conceivably influence the way in which GM130 orients GRASP65 and thereby block binding. Interestingly, a sequence stretch in GRASP65 that is required for GM130 binding roughly corresponds to the sequence stretch identified here as the internal ligand (39). Although the role of specific residues such as Tyr^{198} and Leu^{199} differs in these two interactions, this coincidence could relate to regulation of the internal ligand by GM130.

Based on our findings, the available evidence supports a two-step model for phosphoinhibition of GRASP65 (Fig. 12). First, CDK1 phosphorylates the C-terminal regulatory domain creating a docking site for PLK1. Second, PLK1 binds the docking site, becomes activated, and phosphorylates Ser^{189}, which blocks tethering. Although this likely takes place in M phase, a variation of the model is needed to explain Golgi unlinking in G_2 phase because CDK1 is not yet active. One possibility is that a MEK/ERK cascade creates the PLK1 docking site. MEK/ERK signaling is active in late G_2 and phosphorylates a site in the regulatory domain of GRASP65 (27). The phosphorylation may be mediated by a splice variant of ERK1, ERK1c, which is recruited to the Golgi (46). Interestingly, GRASP55 is also a substrate of ERK and Ser^{189} is conserved, but PLK1 does not bind mitotic GRASP55 (29). Thus, although the mechanism of GRASP55 phosphoregulation may or may not be distinct, GRASP65 is likely phosphorylated on it regulatory domain to create a PLK1 docking site to promote PLK1 phosphorylation of Ser^{189}, which blocks the internal PDZ ligand from binding the PDZ1 groove in another molecule.

Golgi ribbons are primarily evident in higher eukaryotic cells, and this organization converts the compartment from multiple distinct units into a "single-copy" organelle. To ensure equal partitioning at mitosis the Golgi ribbon is fragmented. GRASP proteins are multifunctional, and a version of GRASP is expressed in simpler eukaryotes that lack Golgi ribbons (47, 48). In these cells GRASP is likely involved in cargo secretion by conventional and unconventional pathways (49–53) and may also perform membrane tethering in a simpler reaction such as cisternal elongation. Interestingly, the GRASP phosphorylation site hit by PLK1, Ser^{189}, is apparently only present in cells with Golgi ribbons, and it is only these cell types that express both GRASP isoforms. Thus, the mechanism inducing fragmentation of the Golgi ribbon may have coevolved with the mechanism of Golgi ribbon formation.

Acknowledgments—We thank Steven Truschel for preparing G65-His and $G65^{LK55,56NI}$*-His proteins and Collin Bachert for generating the* $G65^{7XD}$*-GFP-Acta, G65-Myc, His-PDZ1, and His-PDZ2 constructs and both for input into the project including suggestions on the manuscript.*

REFERENCES

1. Misteli, T., and Warren, G. (1995) *J. Cell Sci.* **108,** 2715–2727
2. Lucocq, J. M., Pryde, J. G., Berger, E. G., and Warren, G. (1987) *J. Cell Biol.* **104,** 865–874
3. Jesch, S. A., and Linstedt, A. D. (1998) *Mol. Biol. Cell* **9,** 623–635
4. Kano, F., Takenaka, K., Yamamoto, A., Nagayama, K., Nishida, E., and Murata, M. (2000) *J. Cell Biol.* **149,** 357–368
5. Hidalgo Carcedo, C., Bonazzi, M., Spanò, S., Turacchio, G., Colanzi, A., Luini, A., and Corda, D. (2004) *Science* **305,** 93–96
6. Feinstein, T. N., and Linstedt, A. D. (2007) *Mol. Biol. Cell* **18,** 594–604
7. Colanzi, A., Hidalgo Carcedo, C., Persico, A., Cericola, C., Turacchio, G., Bonazzi, M., Luini, A., and Corda, D. (2007) *EMBO J.* **26,** 2465–2476
8. Puthenveedu, M. A., Bachert, C., Puri, S., Lanni, F., and Linstedt, A. D. (2006) *Nat. Cell Biol.* **8,** 238–248
9. Feinstein, T. N., and Linstedt, A. D. (2008) *Mol. Biol. Cell* **19,** 2696–2707
10. Lucocq, J. M., Berger, E. G., and Warren, G. (1989) *J. Cell Biol.* **109,** 463–474
11. Jesch, S. A., Mehta, A. J., Velliste, M., Murphy, R. F., and Linstedt, A. D. (2001) *Traffic* **2,** 873–884
12. Sütterlin, C., Hsu, P., Mallabiabarrena, A., and Malhotra, V. (2002) *Cell* **109,** 359–369
13. Rabouille, C., and Kondylis, V. (2007) *Cell Cycle* **6,** 2723–2729
14. Barr, F. A., Puype, M., Vandekerckhove, J., and Warren, G. (1997) *Cell* **91,** 253–262
15. Short, B., Preisinger, C., Körner, R., Kopajtich, R., Byron, O., and Barr, F. A. (2001) *J. Cell Biol.* **155,** 877–883
16. Kuo, A., Zhong, C., Lane, W. S., and Derynck, R. (2000) *EMBO J.* **19,** 6427–6439
17. Wang, Y., Satoh, A., and Warren, G. (2005) *J. Biol. Chem.* **280,** 4921–4928
18. Xiang, Y., and Wang, Y. (2010) *J. Cell Biol.* **188,** 237–251
19. Sengupta, D., Truschel, S., Bachert, C., and Linstedt, A. D. (2009) *J. Cell Biol.* **186,** 41–55
20. Bachert, C., and Linstedt, A. D. (2010) *J. Biol. Chem.* **285,** 16294–16301
21. Jesch, S. A., Lewis, T. S., Ahn, N. G., and Linstedt, A. D. (2001) *Mol. Biol. Cell* **12,** 1811–1817
22. Acharya, U., Mallabiabarrena, A., Acharya, J. K., and Malhotra, V. (1998) *Cell* **92,** 183–192
23. Acharya, U., Jacobs, R., Peters, J. M., Watson, N., Farquhar, M. G., and Malhotra, V. (1995) *Cell* **82,** 895–904
24. Wang, Y., Seemann, J., Pypaert, M., Shorter, J., and Warren, G. (2003) *EMBO J.* **22,** 3279–3290
25. Sütterlin, C., Lin, C. Y., Feng, Y., Ferris, D. K., Erikson, R. L., and Malhotra, V. (2001) *Proc. Natl. Acad. Sci. U.S.A.* **98,** 9128–9132
26. Lin, C. Y., Madsen, M. L., Yarm, F. R., Jang, Y. J., Liu, X., and Erikson, R. L. (2000) *Proc. Natl. Acad. Sci. U.S.A.* **97,** 12589–12594
27. Yoshimura, S., Yoshioka, K., Barr, F. A., Lowe, M., Nakayama, K., Ohkuma, S., and Nakamura, N. (2005) *J. Biol. Chem.* **280,** 23048–23056
28. Bisel, B., Wang, Y., Wei, J. H., Xiang, Y., Tang, D., Miron-Mendoza, M., Yoshimura, S., Nakamura, N., and Seemann, J. (2008) *J. Cell Biol.* **182,** 837–843
29. Preisinger, C., Körner, R., Wind, M., Lehmann, W. D., Kopajtich, R., and Barr, F. A. (2005) *EMBO J.* **24,** 753–765
30. Elia, A. E., Cantley, L. C., and Yaffe, M. B. (2003) *Science* **299,** 1228–1231
31. Barr, F. A., Silljé, H. H., and Nigg, E. A. (2004) *Nat. Rev. Mol. Cell Biol.* **5,** 429–440
32. Lowery, D. M., Lim, D., and Yaffe, M. B. (2005) *Oncogene* **24,** 248–259
33. Duronio, R. J., Jackson-Machelski, E., Heuckeroth, R. O., Olins, P. O., Devine, C. S., Yonemoto, W., Slice, L. W., Taylor, S. S., and Gordon, J. I. (1990) *Proc. Natl. Acad. Sci. U.S.A.* **87,** 1506–1510
34. Linstedt, A. D., Jesch, S. A., Mehta, A., Lee, T. H., Garcia-Mata, R., Nelson, D. S., and Sztul, E. (2000) *J. Biol. Chem.* **275,** 10196–10201
35. Nakajima, H., Toyoshima-Morimoto, F., Taniguchi, E., and Nishida, E. (2003) *J. Biol. Chem.* **278,** 25277–25280
36. Macùrek, L., Lindqvist, A., Lim, D., Lampson, M. A., Klompmaker, R., Freire, R., Clouin, C., Taylor, S. S., Yaffe, M. B., and Medema, R. H. (2008) *Nature* **455,** 119–123
37. Golsteyn, R. M., Schultz, S. J., Bartek, J., Ziemiecki, A., Ried, T., and Nigg, E. A. (1994) *J. Cell Sci.* **107,** 1509–1517
38. Tang, D., Yuan, H., and Wang, Y. (2010) *Traffic* **11,** 827–842

39. Barr, F. A., Nakamura, N., and Warren, G. (1998) *EMBO J.* **17,** 3258–3268
40. Zhang, Y., Appleton, B. A., Wiesmann, C., Lau, T., Costa, M., Hannoush, R. N., and Sidhu, S. S. (2009) *Nat. Chem. Biol.* **5,** 217–219
41. Runyon, S. T., Zhang, Y., Appleton, B. A., Sazinsky, S. L., Wu, P., Pan, B., Wiesmann, C., Skelton, N. J., and Sidhu, S. S. (2007) *Protein Sci.* **16,** 2454–2471
42. Hillier, B. J., Christopherson, K. S., Prehoda, K. E., Bredt, D. S., and Lim, W. A. (1999) *Science* **284,** 812–815
43. Penkert, R. R., DiVittorio, H. M., and Prehoda, K. E. (2004) *Nat. Struct. Mol. Biol.* **11,** 1122–1127
44. Birrane, G., Chung, J., and Ladias, J. A. (2003) *J. Biol. Chem.* **278,** 1399–1402
45. Chen, B. S., Braud, S., Badger, J. D., 2nd, Isaac, J. T., and Roche, K. W. (2006) *J. Biol. Chem.* **281,** 16583–16590
46. Shaul, Y. D., and Seger, R. (2006) *J. Cell Biol.* **172,** 885–897
47. Kondylis, V., Spoorendonk, K. M., and Rabouille, C. (2005) *Mol. Biol. Cell* **16,** 4061–4072
48. Behnia, R., Barr, F. A., Flanagan, J. J., Barlowe, C., and Munro, S. (2007) *J. Cell Biol.* **176,** 255–261
49. D'Angelo, G., Prencipe, L., Iodice, L., Beznoussenko, G., Savarese, M., Marra, P., Di Tullio, G., Martire, G., De Matteis, M. A., and Bonatti, S. (2009) *J. Biol. Chem.* **284,** 34849–34860
50. Schotman, H., Karhinen, L., and Rabouille, C. (2008) *Dev. Cell* **14,** 171–182
51. Kinseth, M. A., Anjard, C., Fuller, D., Guizzunti, G., Loomis, W. F., and Malhotra, V. (2007) *Cell* **130,** 524–534
52. Duran, J. M., Kinseth, M., Bossard, C., Rose, D. W., Polishchuk, R., Wu, C. C., Yates, J., Zimmerman, T., and Malhotra, V. (2008) *Mol. Biol. Cell* **19,** 2579–2587
53. Manjithaya, R., Anjard, C., Loomis, W. F., and Subramani, S. (2010) *J. Cell Biol.* **188,** 537–546